Processing and elastic property characterization of porous SiC preform for interpenetrating metal/ceramic composites

Siddhartha Roy, Karl Günter Schell, Ethel Claudia Bucharsky, Pascal Hettich, Stefan Dietrich, Kay A. Weidenmann, Alexander Wanner, Michael J. Hoffmann

Angaben zur Veröffentlichung / Publication details:

Roy, Siddhartha, Karl Günter Schell, Ethel Claudia Bucharsky, Pascal Hettich, Stefan Dietrich, Kay A. Weidenmann, Alexander Wanner, and Michael J. Hoffmann. 2012. "Processing and elastic property characterization of porous SiC preform for interpenetrating metal/ceramic composites." *Journal of the American Ceramic Society* 95 (10): 3078–83. https://doi.org/10.1111/j.1551-2916.2012.05347.x.

Processing and Elastic Property Characterization of Porous SiC Preform for Interpenetrating Metal/Ceramic Composites

Siddhartha Roy,† Karl Günter Schell, Ethel Claudia Bucharsky, Pascal Hettich, Stefan Dietrich, Kay André Weidenmann, Alexander Wanner, and Michael J. Hoffmann*,**

Institute for Applied Materials, Karlsruhe Institute of Technology, 76131 Karlsruhe, Germany

Silicon carbide reinforced aluminum alloy matrix composites offer excellent thermo-mechanical properties and are thus attractive for applications limited by thermal stresses. Open porous silicon carbide preforms are fabricated in this work using polymer wax as pore formers. Two different waxes with different particle size were used to fabricate preforms with different pore structures. Wax content was varied to introduce open porosities up to 64 vol%. Structural characterization was carried out using scanning electron microscopy and micro computed tomography, whereas ultrasound phase spectroscopy was used to determine three longitudinal and three shear elastic constants. The amount of porosity increases with the amount of total wax used. Uniaxial pressing prior to isostatic pressing flattens the pores and as a result the preforms behave transverse isotropically with respect to the press direction. For the same total wax content, while the mixture ratio of two waxes has a minor influence on total porosity, the mixture ratio strongly influences the elastic constants. Optimum elastic constants along all directions are obtained with a mixture of two wax types with a higher content of the larger wax particles.

I. Introduction

Materials for electronic packaging thermal control need to combine high specific stiffness and strength, low coefficient of thermal expansion (CTE), and high thermal conductivity.[1] Silicon carbide particle reinforced aluminum with high ceramic content is among the few materials which satisfy these criteria.[1–3] Interpenetrating composites (IPC) where both matrix and reinforcement are continuous in 3-D offer enhanced mechanical properties in comparison to particle reinforced composites at both room and elevated temperatures.[4] Recently, Roudini *et al.*[5] showed that both CTE and the extent of thermal hysteresis decrease with increasing contiguity of the reinforcement phase. These and the added ability to tailor the phase architecture have resulted in widespread interests in IPCs in last few years.[6]

IPCs with a metallic phase and a ceramic reinforcement are typically fabricated by infiltrating liquid metal into an open porous ceramic preform under external pressure.[7,8] Topology and volume fraction of the reinforcement phase play deciding roles in controlling the properties of the composites.[5,6] Several recent studies have reported the fabrication of open porous SiC preforms for fabrication of IPC. While preceramic polymer binders were used by Thünemann *et al.*[9] and Ma and Yu[10]; Shen *et al.*[11] used ceramic injection molding to fabricate the porous bodies. Based on a preliminary study carried out by Dröschel,[12] we report a simple approach to fabricate open porous SiC preforms by using polyethylene wax as pore formers. Two wax varieties with very different particle sizes were used in different quantities in this study to fabricate SiC preforms with different porosities in the range 45–65 vol% and varying pore morphologies. Structural characterization of the preforms was carried out using scanning electron microscope (SEM) and micro computer tomography (μCT). Ultrasound phase spectroscopy (UPS) was used to perform a first study of the elastic properties of the preforms. Three longitudinal and three shear elastic constants were determined and this throws light on the influence of processing parameters on the elastic anisotropy of the preforms.

To facilitate understanding in the discussion of elastic anisotropy in the fabricated preforms, a very brief description of the general elasticity theory of materials is given in the following and for more complete description we refer to Nye[13] and Hearmon.[14]

Generalized Hooke's law for an anisotropic material is written as:

$$\sigma_{ij} = C_{ijkl} \cdot \varepsilon_{kl} \tag{1}$$

In this equation, σ_{ij} is the stress tensor, ε_{kl} is the strain tensor, and C_{ijkl} is the stiffness tensor. The stiffness tensor, being a fourth order tensor, has 81 components. However, symmetry conditions reduce the number of elastic constants from 81 to 36. Usually, elastic constants are denoted using only two suffixes and expressed in a 6 × 6 matrix form as follows:

$$C_{ij} = \begin{pmatrix} C_{11} & C_{12} & C_{13} & C_{14} & C_{15} & C_{16} \\ C_{21} & C_{22} & C_{23} & C_{24} & C_{25} & C_{26} \\ C_{31} & C_{32} & C_{33} & C_{34} & C_{35} & C_{36} \\ C_{41} & C_{42} & C_{43} & C_{44} & C_{45} & C_{46} \\ C_{51} & C_{52} & C_{53} & C_{54} & C_{55} & C_{56} \\ C_{61} & C_{62} & C_{63} & C_{64} & C_{65} & C_{66} \end{pmatrix} \tag{2}$$

Strain energy considerations of a crystal impose one further restriction $C_{ij} = C_{ji}$, and hence 21 independent elastic constants are necessary for the most anisotropic triclinic system. As the crystal symmetry increases, the number of independent elastic constants decreases, so that in the most symmetric isotropic system only two independent elastic constants, C_{11} and C_{12}, are necessary. Isotropic materials have identical properties along all directions and poly-crystalline solids in the absence of any texture belong to this class. Transverse isotropic materials show rotational symmetry about one axis and the stiffness matrix consists of five independent elastic constants. For rotational symmetry around

T. Ohji—contributing editor

Supported by the German Research Foundation (DFG), under Grant No. RO 4164/1-1

*Member, The American Ceramic Society

**Fellow, The American Ceramic Society

†Author to whom correspondence should be addressed. e-mail: Siddhartha.roy@kit.edu

axis 1 the independent elastic constants are C_{11}, C_{22}, C_{12}, C_{23}, and C_{55}.

II. Experimental Procedure

(1) Processing and Structural Characterization

Ready to press SiC powder "Amperpress Alpha-Silicon Carbide Grade UF-15- Premix" (hereafter named as "Amperpress SiC") and polyethylene waxes "Viscowax" (VW) and "Ceridust" (CD) were used as raw materials. Table I summarizes the names of the suppliers and the characteristics of these raw materials.

To fabricate the preforms three different mixtures with different SiC powder to total wax ratio (in vol%) were made. In each of these three mixture types, the volume fractions of VW and CD were varied to prepare five different mixtures. Plan for fabrication of the porous preforms is schematically shown in Fig. 1.

The dry mixed powder was first uniaxially hand pressed under 40 MPa applied pressure and then cold isostatically pressed under 400 MPa for 90 s. Four tablets from each mixture type were fabricated to check the reproducibility of the process. The green preforms were vacuum dried at 60 °C for 24 h. They were subsequently heated and sintered to fabricate the porous preforms. Melting and pyrolysis of the wax occurred during heating. Both heating and sintering were carried out in argon atmosphere and steps followed during these two processes are shown in Fig. 2. Final preforms were cylindrical in shape with nominal diameter 20 mm and height between 7 and 9 mm.

The amounts of open, closed, and total porosity in each sample were calculated by measuring the density of the samples following Archimedes principle, by immersing in distilled water. For structural analysis, rectangular parallelepipeds (nominal dimensions 8 mm × 5 mm × 5 mm) were cut from the cylinders using a diamond wire saw. The coordinate system used in this work is schematically shown in Fig. 3. The direction parallel to the uniaxial press direction is taken as direction 1 and it also corresponds to the long axis of each rectangular parallelepiped sample. SEM analysis of the preforms was carried out using a SEM ZEISS (Oberkochen, Germany) EVO 50 and μCT analysis was carried out using a CT system of type Y.CT PRECISION from YXLON International GmbH, Hamburg, Germany. For μCT analysis, the voxel side length was in the range 4–5 μm.

(2) Elastic Property Analysis Using Ultrasound Phase Spectroscopy

Only a brief description of UPS is given here and thorough description can be found in literature.[15,16] Continuous, sinusoidal, elastic waves are used in this technique to measure the phase shift of the propagating wave as a function of frequency. The measurements were carried out using a network analyzer (Advantest model 3754A, Advantest, Tokyo, Japan) and two identical broadband ultrasonic longitudinal wave (V122 from Panametrics, Hofheim, Germany, with central frequency 7.5 MHz) and shear wave (V155 from Panametrics with central frequency 5 MHz) transducers. The transducers were attached to opposite faces of the rectangular parallelepiped samples with the help of a water soluble couplant. For both, longitudinal and shear elastic constants the determination of the phase and amplitude spectra were carried out in the range 10 kHz–2 MHz. In a nondispersive specimen of length L, the group velocity V of the propagating wave can be determined following the relation:

$$V = -2\pi \cdot L/m \tag{3}$$

where m is the slope of the phase-frequency spectrum. Once V is known for a particular mode of wave propagation, the appropriate longitudinal and shear elastic constants can be determined according to:

$$C_{ii} = \rho \cdot V^2 \tag{4}$$

where ρ is sample density. For longitudinal elastic constants, i lies between 1 and 3, whereas for shear elastic constants, i is between 4 and 6. In case of shear elastic constants, the

Table I. Description of the Powders Used to Fabricate the Porous Preforms

Material	Supplier	Density (g/cm^3)	Particle size
Amperpress SiC (SiC)	H. C. Starck GmbH, Germany	3.15	<38 μm (35%) >150 μm (3%)
Viscowax 112 (VW)	Innospec Inc., Germany	0.93–0.95	~150 μm
Ceridust 3620 (CD)	Clariant AG, Switzerland	0.96–0.98	7.5–9.5 μm

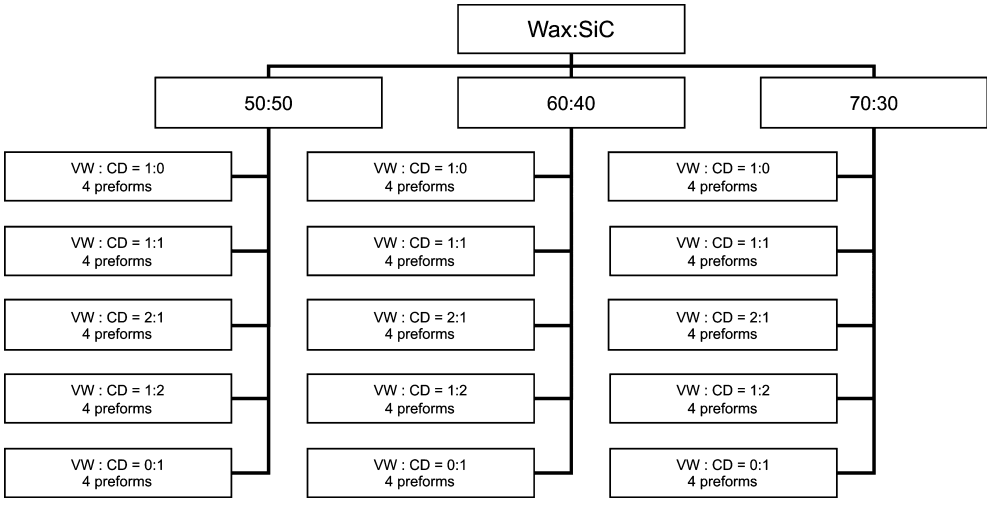

Fig. 1. Schematic plan for fabrication of the porous preforms

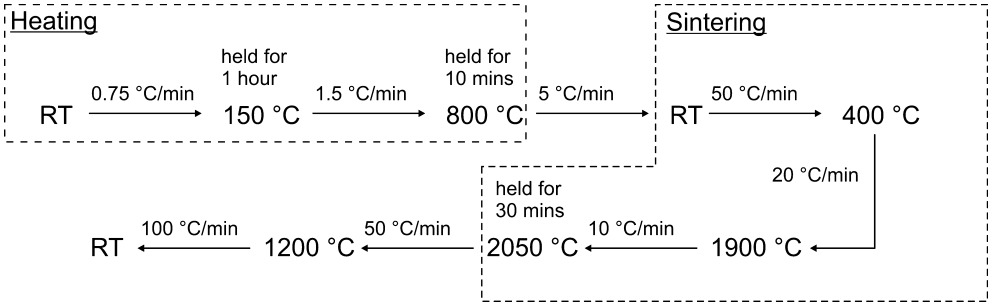

Fig. 2. Steps followed during heating and sintering

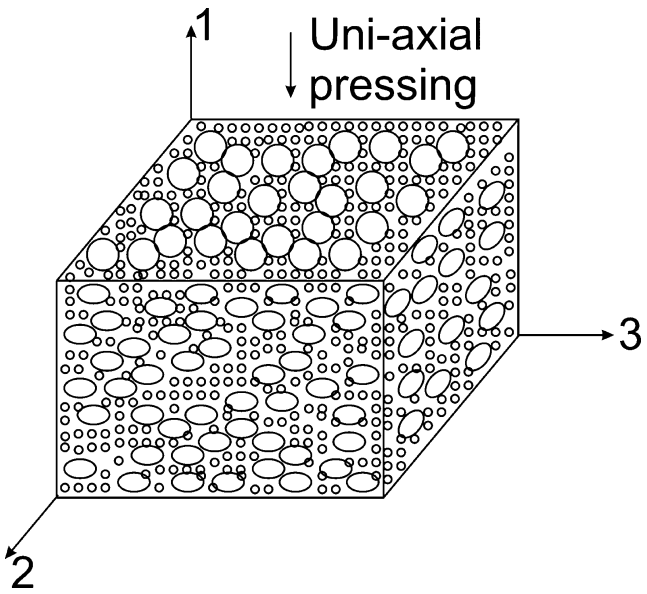

Fig. 3. Schematic representation of the coordinate system used in this work. Direction 1 is parallel to the direction of uniaxial pressing

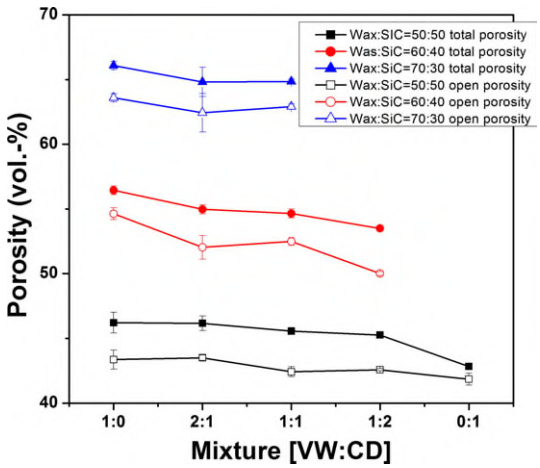

Fig. 4. Variation in total and open porosity as a function of wax: SiC ratio and mixture type. Solid symbols denote total porosity, whereas open symbols denote open porosity

direction of wave propagation is orthogonal to the direction of vibration of the particles of the medium. Each of the three shear elastic constants C_{44}, C_{55}, and C_{66} can be determined using two shear wave velocities V_{xy}[17] (first suffix denotes direction of propagation and second suffix denotes direction of vibration of the medium). For C_{44}, C_{55}, and C_{66}, these sets of velocities are V_{23} and V_{32}, V_{13} and V_{31}, and V_{12} and V_{21}, respectively. For each shear elastic constant in all samples, these six velocities were determined and the average of the corresponding velocities for each constant was used in Eq. (3).

Measurement of elastic constants was carried out on one sample of each batch. The sample with 30 vol% SiC and VW: CD ratio 1:1 in the powder mixture broke during UPS measurement and could not be measured. For both longitudinal and shear elastic constants the measurement of wave velocity was repeated several times to reduce experimental error.

III. Results and Discussions

Figure 4 shows the amounts of total and open porosity as a function of VW:CD ratio for the powder mixtures containing 30, 40, and 50 vol% SiC. In this plot, total porosity is denoted by the solid symbols and open porosity is denoted by open symbols. Data points in the plot correspond to average of 4 samples in each mixture type and the error bars denote one standard deviation. For all mixture types the error bars are very small, suggesting that the results are reproducible. For any mixture type, the difference between the two porosities denotes the amount of closed porosity. Its amount lies in the range 2–3 vol% and as they are not filled during melt infiltration, they will remain as residual porosity in the metal/ceramic composite. In mixtures with high total wax volume content (in 60:40 and 70:30 wax:SiC mixtures) and high CD wax content (VW:CD = 0:1 for 60:40 mixture and VW:CD = 1:2 and 0:1 for 70:30 mixture), the preforms were too fragile after the heating step and could not be used further.

In general, both the amounts of total and open porosity increase with increasing total wax content in the initial mixture. For same total wax content the amount of closed porosity remains relatively constant for different mixture ratios; whereas the amounts of total and open porosity slightly decrease with increasing CD wax content in the mixture. In all preforms the amount of total porosity is 4–6 vol% less than the total wax content in the initial mixture. This may be attributed to the sintering effect.

Figure 5 shows representative SEM images of the porous preforms with various wax contents in the initial mixture. Preforms shown in micrographs (a–c) contain similar porosity and they were made from the 50:50 mixture. The preform shown in the micrograph (d) contains 53 vol% porosity and it was made from the 60:40 mixture with VW to CD wax ratio 1:2. All four micrographs show the face parallel to the direction of uniaxial pressing. The coordinate system is also marked in each image, where the vertical direction is the uniaxial press direction. It can be observed that for the same total wax content the mixture ratio strongly influences the pore structure. Pores resulting from bigger, round shaped VW are oval to spherical in shape. Sizes of these pores are similar to the diameter of the original VW particles. Uniaxial pressure applied prior to isostatic pressing deforms the pores and flattens them along the direction of applied pressure. SiC regions between the large VW pores are densely sintered. However, several cracks are observed in these regions

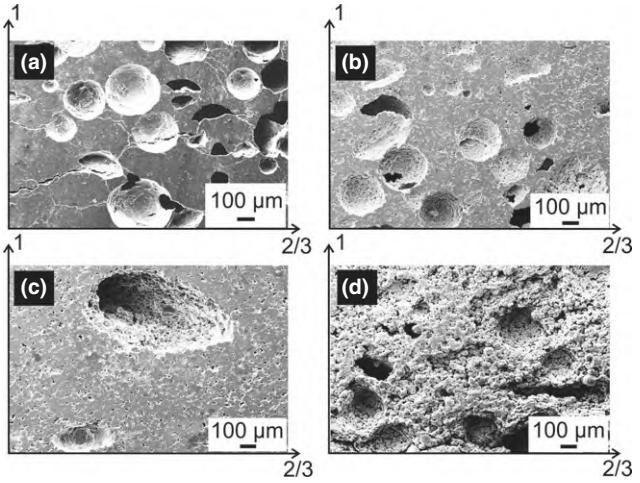

Fig. 5. SEM images of the porous preforms: (a) total porosity 46 vol% and VW:CD = 1:0; (b) total porosity 47 vol% and VW:CD = 2:1; (c) total porosity 43 vol% and VW:CD = 0:1; (d) total porosity 53 vol% and VW:CD = 1:2. In these images the uniaxial press direction is along the vertical direction. The coordinate system is marked in each image.

connecting adjacent VW pores. During heating of the preforms, the wax expands as it melts and this gives rise to the through cracks in the densely packed SiC region between the large pores. These cracks act as channels through which the molten wax flows out. In preforms consisting of mixture of VW and CD a tri-modal pore structure is observed: (a) oval to round shaped large pores resulting from VW, (b) very fine pore network resulting from individual CD particles, and (c) few very large pores (in mm range) resulting from agglomerates of CD formed during initial mixing of the powders. The fine network pore structure allows sufficient space for the molten wax to flow out during heating and as a result cracks between the VW pores, present in preforms with only VW, are no more visible here. Finally, in preforms with only CD a bimodal pore structure is observed – fine pores resulting from CD and large pores from CD agglomerates. Also, no cracks are observed between the pores. As can be seen in Fig. 5(c), large pores resulting from CD agglomerates are also oriented perpendicular to the direction of uniaxial pressing.

Figure 5(d) shows that too high CD content in the mixture, however, detrimentally affects the structure of the preforms. The SiC particles are no more densely sintered and are only connected by mere point contacts. At high volume fraction of porosities the very fine interpenetrating pore structure, thus makes the preform too fragile to be self-supporting. This also explains the inability in processing usable preforms with higher total wax and CD content.

Figure 6 shows typical orthogonal slices obtained from μCT analysis for two different preform types with similar

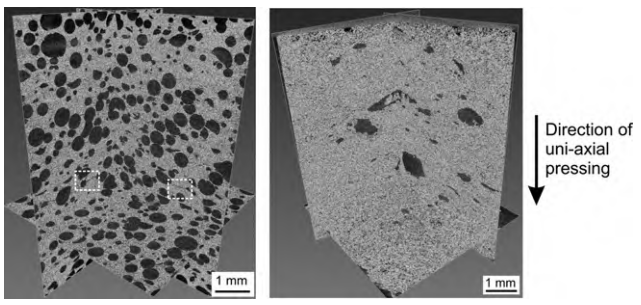

Fig. 6. Representative orthogonal slices of the preforms obtained from μCT analysis. Porosity 46 vol% and VW:CD = 1:0 (left) and porosity 43 vol% and VW:CD = 0:1 (right). The direction of uniaxial pressing is shown by the arrow.

total porosities. The image on the left-hand side corresponds to the sample whose SEM image is shown in Fig. 5(a), whereas the right-hand side image corresponds to the sample shown in Fig. 5(c). The direction of uniaxial pressing prior to cold isostatic pressing is shown by the arrow. These images allow observing the structure of the preforms in 3-D, albeit at a lower resolution than the SEM images. In these gray scale images the pores are black, whereas the SiC regions are gray. Flattening of the large pores resulting from round VW particles and CD agglomerates along the uniaxial press direction is clearly visible in both images. Cracks observed during SEM analysis between the large pores in the VW sample are also visible in the μCT image (two such cracks are marked with white bounding boxes). At several locations in the VW preform two large pores have joined to form larger pores. Probably this resulted from adjacently lying VW particles after mixing of the powders. Large pores several millimeter in diameter resulting from CD agglomerates can also be seen in the right-hand side image.

As discussed by Cumberland,[18] pore shapes in porous ceramic bodies fabricated using pore formers as space holders depend upon the ratio of the ceramic particle diameter to the pore former diameter. Considering the phase with higher volume fraction as the matrix phase, it was shown that interpenetrating pore structure is obtained when the diameter ratio between the second phase and the matrix phase becomes less than 0.154. The degree of interlinking increases with increasing volume fraction of the second phase. When this diameter ratio becomes more than 0.732, the matrix phase surrounds the larger second phase particles. As discussed by Dröschel,[12] when the diameter of the pore forming particles is larger than SiC (as with VW), the SiC powders surround the pore formers and the pore shape depends upon the shape of the pore former. When the pore formers are smaller than the SiC particles (as with CD), the pore formers fill the gap between the particles and the pore shape depends upon the size and shape of the gap. Therefore, in performs with VW, the pore shape replicates the initial shape of wax particles, whereas pores resulting from CD are smaller and more irregular in shape. But in general, both wax types provide a homogenous pore distribution throughout the green compacts. As shown in Figs. 5 and 6, the smaller CD particles permit better interconnectivity in comparison to performs with only VW as pore former. Using only one wax type (VW:CD = 1:0 and 0:1), extremities of pore morphologies are obtained. By fabricating performs with mixtures of the two wax types (as in VW:CD = 2:1, 1:1, and 1:2) it is possible to fabricate preforms with tailor-made morphology and wide range of properties.

Both Figs. 5 and 6 further show that the initial applied 40 MPa uniaxial pressure plays a deciding role in controlling the pore structure, and its effect is not nullified even by subsequent 10 times larger isostatic pressure.

Figure 7 shows typical phase and amplitude spectra for longitudinal and shear elastic constants in one sample. In these plots the phase spectra are denoted by the red lines, whereas the amplitude spectra are denoted by the blue lines. For longitudinal waves the amplitude spectra show similar trend. After a sudden drop at around 750 kHz, the spectra oscillate in a complex manner at almost constant amplitude. In case of shear waves, the amplitude keeps on decreasing with increasing frequency. For C_{55} and C_{66} the amplitudes drop below measureable limit at higher frequency. The double sided black arrows on each phase spectrum denote the regions over which the slope was determined for determination of elastic constants following Eq. 3. In all cases, the phase spectra are linear over the complete measured frequency range. This denotes that the porous preforms are nondispersive and measured wave velocity is independent of frequency.

Figure 8 plots the dependence of longitudinal and shear elastic constants on the VW:CD mixture ratio in preforms

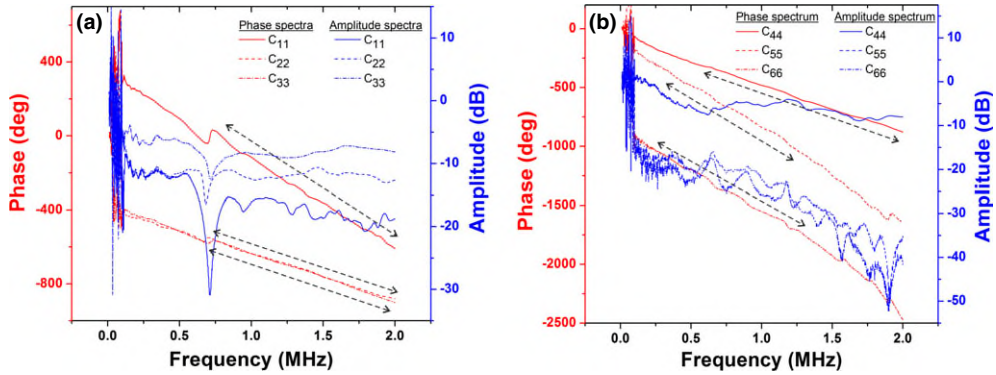

Fig. 7. Typical phase and amplitude spectra for (a) longitudinal and (b) shear elastic constants in one sample. In these plots the red lines denote the phase spectra, whereas the blue lines denote the amplitude spectra.

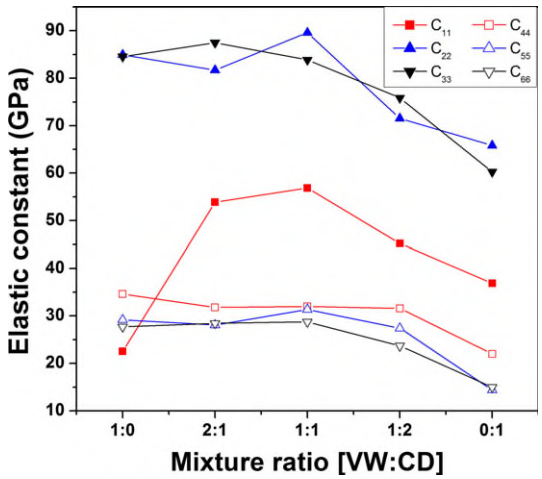

Fig. 8. Effect of VW:CD mixture ratio on the longitudinal and shear elastic constants in preforms fabricated using 50:50 mixture of wax:SiC.

fabricated from 50:50 wax:SiC powder mixture. Qualitatively similar trend was also observed for 60:40 wax:SiC mixture. Only two samples could be measured in the 70:30 wax:SiC type and hence no trend could be determined. The plot shows that for all mixture types the longitudinal elastic constants follow the trend $C_{11} < C_{22} \approx C_{33}$. Correspondingly, for shear elastic constants, $C_{44} > C_{55} \approx C_{66}$. Hence, the symmetry of the porous preforms is transverse isotropic with respect to the direction of uniaxial pressing along direction 1 in Fig. 3. This is a direct consequence of the shapes of the pores in the preforms. Effect of porosity on the properties of ceramic materials has been described in detail in monographs written by Rice.[19,20] While density depends only on the total amount of porosity in the material, elastic constants depend both on the total amount and the character (amount or degree of open and closed porosity, pore size, pore shape, minimum solid area etc.) of the pores. Porous bodies with equiaxed pores display isotropic elastic behavior. Plots of relative elastic constant (property of the porous body normalized by the corresponding property of the pore free body) in log scale against porosity in linear scale up to a certain intermediate porosity level typically show a linear region with a constant slope $-b$, with b typically ranging between 2 and 7.[19] For nonequiaxed pore shapes the materials display anisotropic character. Andersson[21] derived relations for the effect of ellipsoidal pores on Young's modulus of porous bodies. It was found that b is strongly dependent upon the aspect ratio k (=half of minor axis/half of major axis) and orientation (φ) of the pores with respect to the direction of stress application, but independent of the pore size. When the long axis of the pore is normal to the stress axis, b becomes infinitely large as k approaches zero, and tends toward unity as k becomes large. For pores with long axis parallel to the direction of applied stress, b was only marginally dependent upon the aspect ratio and ranged between 2.1 and 2.9. Penny shaped cracks with no volume represent the most extreme case ($k = 0$) and that results in the steepest drop in stiffness with porosity ($b = \infty$) when stress is applied normal to their long axis. In another work for open cell foams with elongated pores, Huber and Gibson[22] derived expressions for mechanical properties along and transverse to the long axis of the pores. Young's modulus was found to be strongly dependent upon the cell dimensions, with an aspect ratio of 2 resulting in almost 8 times higher modulus along the long axis.

Figure 6 (left) shows that the VW pores have been flattened along direction 1. In the plane normal to the press direction (2–3 plane) the pores have spherical cross-section. Hence, in preforms with VW wax the VW pores has an ellipsoidal pore structure with the long axis of the ellipsoid normal to direction 1. The applied uniaxial pressure has also flattened the large pores resulting from CD agglomeration in direction 1. These explain the transverse isotropic symmetry of the preforms and reduced stiffness along direction 1. Although for same wax:SiC powder ratio the mixture ratio between VW and CD has a minor influence on total and open porosity (Fig. 4), Fig. 8 clearly shows that for the same amount of porosity the VW:CD ratio strongly influences the elastic constants. The influence being most prominent for C_{11}. For preforms with only VW, C_{11} is significantly less than C_{22} and C_{33}. This can be attributed to the presence of the long through cracks perpendicular to the press direction in this preform type. As derived by Andersson,[21] normal to the long axis of closed cracks significant stiffness reduction takes place and this has also been experimentally shown by Wanner.[23] With increasing CD content, C_{11} first increases up to a VW:CD ratio 1:1. At even higher CD content the elastic constants along all directions show a decreasing trend. This can probably be attributed to the large millimeter size pores present in high-CD preforms.

The varying pore morphologies in the preforms from different mixture ratios of the two wax types have resulted in significant variation in their elastic constants. This results from the interaction between different pore shapes, sizes, and orientations. For a thorough understanding of the effect of porosity and pore morphology on the elastic anisotropy, preforms with varying porosities need to be studied. This will be carried out in our future work.

The thorough 2-D and 3-D structural characterization as well as the first study of elastic behavior carried out in this work allow identifying the parameters to fabricate preforms with optimal microstructure for interpenetrating metal/ceramic composites. Preforms consisting of only one type of wax (either VW or CD) have limitations. While only VW

preforms have long cracks through the dense SiC regions joining the large pores (hence significantly reducing C_{11} in comparison to C_{22} and C_{33}), with high-CD content stiffness decreases along all directions. The current study shows that preforms with optimum elastic properties along all directions are obtained with a mixture of two wax types, with higher volume content of the larger VW wax. To identify the optimum processing parameters, the applied uniaxial pressure needs to be varied for investigating its exact influence on the extent of anisotropy. In addition, the different pore structures in various preforms may influence the internal load transfer and thermal properties of the final infiltrated IPC. These will be analyzed in subsequent studies.

IV. Conclusions

Open porous SiC preforms with porosity in the range 45–65 vol%. were fabricated using polymer wax as pore formers. Two different wax types were used and their total quantities as well as the mixture ratios were varied to fabricate preforms with different pore structures. Structural characterization of the preforms was carried out using SEM and μCT; whereas three longitudinal and three shear elastic constants were determined using UPS.

Following conclusions are drawn:

1. Both open and total porosity increased with the total amount of wax used. For same total wax content the mixture ratio of the two wax types has a negligible influence on total porosity
2. Uniaxial pressure applied prior to isostatic pressing flattens the pores along the press direction. This renders the preforms to behave transverse isotropically with respect to the press direction. Both longitudinal and shear elastic constants along the press direction are softer than those perpendicular to the press direction.
3. Type of wax mixture has a pronounced influence on the preform elastic properties. Preforms made from only one wax type show reduced elastic constants. Optimum elastic constants along all directions are obtained in preforms made from a mixture of the two wax types with a higher content of larger pore formers.

Acknowledgment

The authors thank TER HELL & CO. GmbH for providing them with the polymer waxes free of cost.

References

[1]C. Zweben, "Advances in Composite Materials for Thermal Management in Electronic Packaging," *JOM*, **50**, 47–51 (1998).

[2]C. Zweben, "Metal-Matrix Composites for Electronic Packaging," *JOM*, **44**, 15–23 (1992).

[3]B. G. Kim, S. L. Dong, and S. D. Park, "Effects of Thermal Processing on Thermal Expansion Coefficient of a 50 vol.% SiC_p/Al Composite," *Mater. Chem. Phys.*, **72**, 42–7 (2001).

[4]M. Kouzeli and D. C. Dunand, "Effect of Reinforcement Connectivity on the Elasto-Plastic Behavior of Aluminum Composites Containing Sub-Micron Alumina Particles," *Acta Mater.*, **51**, 6105–21 (2003).

[5]G. Roudini, R. Tavangar, L. Weber, and A. Mortensen, "Influence of Reinforcement Contiguity on the Thermal Expansion of Alumina Particle Reinforced Aluminum Composites," *Int. J. Mat. Res.*, **101**, 1113–20 (2010).

[6]A. Mortensen and J. Llorca, "Metal Matrix Composites," *Annu. Rev. Mater. Res.*, **40**, 243–70 (2010).

[7]S. Roy, J. Gibmeier, V. Kostov, K. A. Weidenmann, A. Nagel, and A. Wanner, "Internal Load Transfer in a Metal Matrix Composite with a Three-Dimensional Interpenetrating Structure," *Acta Mater.*, **59**, 1424–35 (2011).

[8]A. Mattern, B. Huchler, D. Staudenecker, R. Oberacker, A. Nagel, and M. J. Hoffmann, "Preparation of Interpenetrating Ceramic-Metal Composites," *J. Eur. Ceram. Soc.*, **24**, 3399–408 (2004).

[9]M. Thünemann, O. Beffort, S. Kleiner, and U. Vogt, "Aluminum Matrix Composites Based on Preceramic-Polymer-Bonded SiC Preforms," *Compos. Sci. Technol.*, **67**, 2377–83 (2007).

[10]Q.-s. Ma and X.-d. Yu, "Low Temperature Fabrication and Characterisation of Porous SiC Ceramics Using Polycarbosilane as Binder," *Key Engg. Mater.*, **336–338**, 1090–2 (2007).

[11]X. Shen, S. Ren, X. He, M. Qin, and X. Qu, "Study on Methods to Strengthen SiC Preforms for SiC_p/Al Composites by Pressureless Infiltration," *J. Alloy. Compd.*, **468**, 158–63 (2009).

[12]M. Dröschel, M. J. Hoffmann, R. Oberacker, W. Schaller, Y. Y. Yang, and D. Munz, "SiC-Ceramics with Tailored Porosity Gradients for Combustion Chambers," *Key Eng. Mater.*, **175–176**, 149–62 (2000).

[13]J. F. Nye, *Physical Properties of Crystals*. Oxford Science Publications, New York, 1985.

[14]R. F. S. Hearmon, *An Introduction to Applied Anisotropic Elasticity*. Oxford University Press, London, 1961.

[15]A. Wanner, "Elastic Modulus Measurements of Extremely Porous Ceramic Materials by Ultrasonic Phase Spectroscopy," *Mater. Sci. Eng., A*, **A248**, 35–43 (1998).

[16]S. Roy, J.-M. Gebert, G. Stasiuk, R. Piat, K. A. Weidenmann, and A. Wanner, "Complete Determination of Elastic Moduli of Interpenetrating Metal/Ceramic Composites Using Ultrasonic Techniques and Micromechanical Modelling," *Mater. Sci. Eng., A*, **A528**, 8226–35 (2011).

[17]J. L. Rose, *Ultrasonic Waves in Solid Media*. Cambridge University Press, Cambridge, UK, 1999.

[18]D. J. Cumberland and R. J. Crawford, *The Packing of Particles*. Elsevier, Amsterdam, 1987.

[19]R. W. Rice, *Porosity of Ceramics*. Marcel Decker, Inc., New York, 1998.

[20]R. W. Rice, "The Porosity Dependence of Physical Properties of Materials: a Summary Review," *Key Eng. Mater.*, **115**, 1–20 (1996).

[21]C. A. Andersson, "Derivation of the Exponential Relation for the Effect of Ellipsoidal Porosity on Elastic Modulus," *J. Am. Ceram. Soc.*, **79**, 2181–4 (1996).

[22]A. T. Huber and L. J. Gibson, "Anisotropy of Foams," *J. Mater. Sci.*, **23**, 3031–40 (1988).

[23]A. Wanner, "Elastic Properties of Porous Structural Ceramics Produced by Plasma Spraying," *Mater. Res. Soc. Symp. Proc.*, **521**, 45–50 (1998). □